Drug Design, Development and Therapy

Dovepress
Taylor & Francis Group

Open Access Full Text Article

ORIGINAL RESEARCH

Yi-Fei-Tong-Bi Decoction Alleviates Bleomycin Induced Pulmonary Fibrosis in Mice

Kui Du[1,*], Xingjian Wen[2,3,*], Jie Zhu[1], Rui Liang[2,3], Lu Wang[1], Na Li[2,3], Qinghua Zou[1]

[1]Department of Rheumatology and Immunology, First Affiliated Hospital of Army Medical University, Chongqing, People's Republic of China; [2]Chongqing Academy of Chinese Materia Medica, Chongqing, People's Republic of China; [3]Chongqing College of Traditional Chinese Medicine, Chongqing, People's Republic of China

*These authors contributed equally to this work

Correspondence: Qinghua Zou, Department of Rheumatology and Immunology, First Affiliated Hospital of Army Medical University, No. 29, Gaotan Yanzheng Street, Shapingba District, Chongqing, 400038, People's Republic of China, Email zouqinghua318@tmmu.edu.cn; Na Li, Sichuan-Chongqing Joint Key Laboratory of Innovation of New Drugs of Traditional Chinese Medicine, Chongqing Academy of Chinese Materia Medica, No. 34 Nanshan Road, Nan'an District, Chongqing, 400065, People's Republic of China, Email lina@cqacmm.com

Background: Fei-Bi decoction, a Chinese ancient experience decoction collected in the book of Bianzhenglu (Syndrome Differentiation Record). Based on Fei-Bi Decoction, Yi-Fei-Tong-Bi decoction (YFTBD) is developed and has a significant effect in the treatment of pulmonary fibrosis. However, the underlying mechanisms of YFTBD affects pulmonary fibrosis remain to be elucidated.

Purpose: To investigate the protective effect and the underlying mechanism of YFTBD on bleomycin-induced pulmonary fibrosis in mice.

Methods: The chemical components of water extract of YFTBD were analyzed by combining the high performance liquid chromatography (HPLC) coupled with mass spectrometry (MS). A mouse model was established by intratracheal injection of bleomycin, and the effects of YFTBD were evaluated through pathological staining, immunohistochemistry analyses, and Enzyme-Linked Immunosorbent Assay (ELISA). Subsequently, the effect of YFTBD on the gut microbiota of mice was analyzed by 16S rRNA high-throughput gene sequencing.

Results: Compared with the model group, the survival rate and lung coefficient of mice with pulmonary fibrosis were increased after the intervention of YFTBD, the pathological morphology of lung tissue was improved, and the expression of the inflammatory factor levels were decreased. The expression of α-SMA, TGF-β1, p21, and p16 senescence-related proteins was significantly down-regulated. The expression of Smad7 and PGC-1α senescence-related proteins was significantly up-regulated. Meanwhile, gut microbiota analysis showed that YFTBD could induce changes in the abundance of *Alloprevotella, unclassified Muribaculaceae*, and *Lachnospiraceae* NK4A136 group.

Conclusion: Our findings suggest that YFTBD could alleviate the bleomycin-induced pulmonary fibrosis in mice via regulating TGF-β1/Smad signaling pathway, inflammation and gut microbiota. It provides experimental evidence and a theoretical basis for the application of YFTBD in pulmonary fibrosis.

Keywords: Yi-Fei-Tong-Bi decoction, pulmonary fibrosis, collagen, cell senescence, gut microbiota

Introduction

Pulmonary fibrosis is a common fibrotic pulmonary interstitial disease. The pathological changes are disseminated alveolitis, pulmonary interstitial inflammation and interstitial fibrosis.[1] The clinical manifestations are progressive dyspnea, dry cough and fatigue.[2] Pulmonary fibrosis is an end-stage change in many interstitial lung diseases, and the average life expectancy after diagnosis is only 3 years.[3] The increasing incidence of pulmonary fibrosis has increased the medical burden.[4] Therefore, the development of safe and reliable drugs has important clinical value for improving the prognosis of patients with pulmonary fibrosis.

The ideal intervention for treating interstitial lung disease (ILD) is still lacking to this day. Although pirfenidone and nintedanib have been shown to slow disease progression and improve the quality of life for some patients. They are not the ultimate solution for curing the disease. Meanwhile, their effectiveness varies among individuals, and some patients

Received: 13 January 2025
Accepted: 13 April 2025
Published: 15 May 2025

may experience side effects.[5–7] Accumulated evidence found that the notable adverse effects associated with nintedanib, which causing diarrhea with rate of 61.5% or 66.9%.[8] Previous studies systematically analyzed the clinical efficacy of traditional Chinese medicine (TCM) in treating ILD and further summarized the potential mechanisms, including alleviating oxidative stress,[9–16] inhibiting inflammation,[14,17] inhibiting epithelial-mesenchymal transition,[15,18–20] and inhibiting myofibroblast activation.[21,22] In recent years, numerous relevant studies have demonstrated that the gut microbiota is closely associated with pulmonary fibrosis.[23] The gut microbiota and their metabolites can modulate the onset and progression of pulmonary fibrosis via the "gut-lung axis".[24] In traditional Chinese medicine, there exists the theory of "the lung and the large intestine are interior-exterior related". Lung and intestine are interrelated and influence each other in physiology and pathology, and can be treated jointly in treatment.[25] Exploring traditional Chinese medicine preparations for the treatment of interstitial lung disease may provides new hope and opportunity.

Bianzhenglu (Syndrome Differentiation Record) formulates the Fei-Bi Decoction based on the etiology of lung obstruction resulting from deficiencies in lung and spleen qi. The primary treatment principles focus on strengthening the spleen and benefiting the lungs, as well as nurturing the earth to generate metal. This decoction is indicated for addressing symptoms associated with qi deficiency leading to lung obstruction, which include persistent cough, chest tightness, continuous phlegm expectoration, a sensation of fullness and distension in the upper abdomen, and difficulty achieving normal bowel movements. Based on Fei-Bi Decoction, Yi-Fei-Tong-Bi decoction (YFTBD) is developed. It is an effective and experiential prescription for the clinical treatment of pulmonary fibrosis, which can improve the pulmonary symptoms of pulmonary fibrosis such as chest tightness, wheezing and cough. However, the molecular mechanism of YFTBD improving pulmonary fibrosis progression remains unclear. Therefore, the aim of this study is to investigate the effects of YFTBD on bleomycin-induced pulmonary fibrosis in mice and the underlying mechanisms, in order to provide theoretical support for the clinical use of YFTBD in the treatment of pulmonary fibrosis.

Materials and Methods

Drugs

The following drugs were used in this study: bleomycin hydrochloric for injection (ant-zn-1, InvivoGen) and nintedanib esilate soft capsules (HJ20170355, 150 mg/capsule, Catalent Germany Eberbach GmbH). YFTBD consists of 11 Chinese herbs, which were purchased from and identified by Chongqing Shangyao Huiyuan Pharmaceutical Co., Ltd. (Chongqing, China). All herbs were in line with the standards listed in the National Pharmacopoeia of China. YFTBD was taken 1 time the conventional dose (Huangqi/*Astragalus membranaceus* (Fisch). Bge. var. *mongholicus* (Bge). Hsiao 30 g, Dangshen/*Codonopsis pilosula* (Franch). Nannf. 15 g, Fuling/*Poria cocos* (Schw). Wolf 15 g, Danshen/*Salvia miltiorrhiza* Bge. 15 g, Baizhu/*Atractylodes macrocephala* Koidz. 12 g, Xingren/*Prunus armeniaca* L. var. *ansu* Maxim. 12 g, Jiegeng/*Platycodon grandiflorus (Jacq). A.DC*. (PG) 12 g, Chuanxiong/*Ligusticum chuanxiong* Hort. 12 g, Danggui/*Angelica sinensis* (Oliv). Diels 12 g, Wuweizi/*Schisandra chinensis* (Turcz). Baill 6 g, Gancao/*Glycyrrhiza uralensis* Fisch. 9 g) and soaked for 30 min in 16000 mL ultrapure water. Then, two rounds of reflux extraction were performed. The first time: the drug is heated and decocted for 1 h, then the filtrate is poured out and filtered with 400 mesh gauze. The second time: add 1300 mL ultrapure water to the residue and continue to decoction for 1 h, then pour out the liquid and filter with 400 mesh gauze. Subsequently, the twice filtered liquid was mixed and centrifuged for 10 min by 5000 ×g centrifuge. After removing the precipitation, the supernatant of the liquid was obtained. The liquid is further concentrated and kept at a volume of 150 mL to achieve a liquid concentration of 1 g/mL, which was stored in the refrigerator at 4°C for use.

HPLC-MS

Take 20 mL of the traditional Chinese medicine decoction and put it into a 50 mL liquid separation funnel. Subsequently, add 20 mL of petroleum ether, shake vigorously and mix thoroughly. Allow the liquid to separate and retain the aqueous phase. Then, add petroleum ether once again for washing. Subsequently, accurately measure 5 mL of the aqueous solution, evaporate the solvent until dry, dissolve the residue with 20% acetonitrile, transfer it to a 10 mL volumetric flask, add 20% acetonitrile to a constant volume, and shake well. The sample was passed through YMC-Pack ODS-AQ

(5 μm, 4.6*250 mm) with the mobile phase consisted of acetonitrile (A) and an aqueous solution containing 1% tetrahydrofuran and 0.05% phosphoric acid (B) at a detection wavelength of 260 nm for HPLC signals. The separation was achieved using a gradient elution program as follows: 0–15 min: 12% A; 15–60 min: 9% A. The control solution and the test solution were injected into the liquid chromatograph with 10 μL each.

Animal Grouping, Modeling and Dosing

Fifty-eight male C57BL/J6 mice (20–23 g, 7 weeks) were purchased from Hunan Slack Jingda Experimental Animal Co., Ltd with License No. SCXK (Hunan) 2019–0004. The mice were kept in a suitable feeding environment with 12-h light/dark cycle, and free access to both water and food. All animal experiments were conducted in accordance with the standard procedures, and were approved by the Experimental Animal Welfare Ethics Committee of Chongqing Academy of Traditional Chinese Medicine (Certificate of Approval No: ZJS2023-02). After one week of adaptive feeding, the mice were randomly divided into 5 groups, including the control group (control, n=10), model group (model, n=12), nintedanib group (NIB, n=12), YFTBD group (YFTBD, n=12) and nintedanib+YFTBD group (NIB+YFTBD, n=12). Referring to the previous literature,[26–28] the model of pulmonary fibrosis was induced by a single intratracheal injection of 3 mg/kg bleomycin in mice, and the same amount of normal saline was injected into the trachea of mice in the normal group.

After 1 day of intratracheal instillation, YFTBD and/or nintedanib were administered daily by gavage for continue 4 weeks. The mice in YFTBD and NIB+YFTBD groups were respectively administered intragastrically with 19.5 g/kg/d (equivalent to 1 time the clinical dose) of YFTBD, while the mice in NIB and NIB+YFTBD groups were given intragastric administration of 9.75 mg/kg/d nintedanib (equivalent to 1 time the clinical dose). Simultaneously, the normal group and the model group were administered the same volume of normal saline daily. The number of surviving mice in each group was tallied daily during administration and euthanized on the day 28 after endotracheal injection.

Serum Isolation and Detection of Indicator

On day 28, after the last intragastric administration for 9 h, mice were anesthetized by intraperitoneal injection of 2% pentobarbital sodium (35 mg/kg). Then the blood was collected through the fundus venous plexus, the serum was separated and placed in the refrigerator at −80°C for use. Subsequently, the concentrations of IL-1β, IL-6 and TNF-α in serum of mice were detected by enzyme-linked immunosorbent assay (ELISA) kits, which were purchased from Jiangsu Enzyme Immunity Industry Co., Ltd. (Jiangsu, China).

Tissue Collection and Morphological Observation

After blood collection, mice were finally euthanized. Then the lungs were separated and weighed. The lung coefficient was calculated (lung coefficient = lung wet mass (mg)/ body weight (g)× 100%). The left lung of mice was fixed in 4% paraformaldehyde for 24 h, then dehydrated and transparent, paraffin embedded, and sliced. HE staining and Masson staining were performed according to the procedure of the corresponding kits. Finally, the histopathological and morphological changes were observed under a light microscope (Olympus CX31, Japan). The positive expression of Masson staining was quantitatively analyzed using the Image J software (Version 1.54f, USA) and the average optical density (AOD) value was calculated. AOD value = cumulative optical density value/positive pixel area.

Determination of Hydroxyproline Content in Lung Tissue

The middle lobe of the right lung was rinsed with normal saline at 4°C, the excess water was removed with filter paper, and the content of hydroxyproline in the lung tissue was measured by a hydroxyproline quantification assay kit (A030-2, Nanjing Jiancheng Bioengineering Institute, China) after lung mass was weighed. Using known hydroxyproline as standard curve, the content of hydroxyproline in lung tissue was determined to evaluate the metabolic situation of collagen.

Immunohistochemistry Analyses

The expression of α-SMA, TGF-β1, Smad7, p21, and p16 in lung tissues of each group was detected by immunohistochemical staining after paraffin embedding and section. Immunohistochemistry was executed as described earlier.[29] Five visual fields were randomly selected from each section for observation under high power microscope. The

expression in the positive regions was quantitatively analyzed using the Image J software (Version 1.54f, USA) and AOD was calculated.

16S rRNA High-Throughput Gene Sequencing

The day prior to the euthanasia of the mice, five samples from each group were randomly selected for fecal DNA extraction and analysis of gut microbiota diversity. Total DNA was extracted using a DNA extraction kit, with purity and concentration assessed via Nano Drop 2000. Primers targeting the 16S rRNA V3-V4 region (338F: 5′-ACTCCTACGGGAGGCAGCAG-3′; 806R: 5′-GGACTACHVGGGTWTCTAAT-3′) were employed for PCR amplification. The resulting PCR products underwent purification and quantification utilizing appropriate kits based on their concentrations. Following established protocols, library construction was performed using the NEXTFLEX Rapid DNA-Seq Kit, with sequencing conducted on the Illumina MiSeq PE300 platform. The sequencing data were analyzed on the BMKcloud platform (Biomarker Technologies, Beijing, China), encompassing alpha diversity analysis, beta diversity analysis, community structure examination, Linear discriminant analysis (LDA) coupled with effect size (LEfSe) analysis.

Statistical Analysis

Using GraphPad Prism 9.0 statistical software (San Diego, USA) to analyze the experimental data. All experiments in this study were replicated independently at least five times. Measurement data were expressed as mean ± standard deviation (mean ± SD). Statistical analysis was performed using Student's *t*-test was used for comparisons between two groups, whereas one-way analysis of variance (ANOVA) was utilized for comparisons among multiple groups, with 95% confidence interval. $P < 0.05$ was considered as statistically significant.

Results

The Phytochemical Composition of YFTBD

It shows the total ion chromatogram (TIC) (Figure 1A and B), which was generated by comparison with standard materials, chemical data in the mass spectral library mzCloud, relevant literature searches and the TCMSP database (https://old.tcmsp-e.com/tcmsp.php). We found that the primary components of YFTBD were Cryptotanshinone, dihydrotanshinone, Tanshinone I, salvianolic acid CBIA, Angelicolactone A, Angelicolactone dilactone, Ferulic acid, atractylodes I, II, and III, codonetyne side, codonetine, liquiritin, glycyrrhizin V, ligustilide, vanillic acid, 3-o-β-D-glucopyranosyl platycodon saponin, amygdalin, sakurin, isoastragalus saponin I, Astragalus saponin II, IV, schisandrin, schisandrin B, schisandrin A, schisandrin A, etc (Supplementary Tables 1–3).

YFTBD Alleviates Lung Injury and Collagen Deposition in Mice

HE staining results (Figure 2A) showed that no alveolar inflammatory exudation and fibrosis lesions were found in the lung tissue of mice in the normal group, and the alveolar structure was clear and complete. The number of interstitial cells in the lung of mice in the model group increased, the proliferation of fibrous tissue increased, and the lung tissue was severely damaged. In mice treated with YFTBD, the fibrosis of lung tissue was alleviated, the lung tissue structure was clear, and the lung interstitium was slightly increased.

Masson staining results (Figure 2B) showed that the alveoli in the lungs of mice in the control group were evenly distributed, with no obvious fibrosis and no obvious inflammatory cell infiltration. Compared with the control group, bleomycin-induced lung tissue structure disorder, blue collagen deposition in the lung interstitium, atrophy and collapse of some alveolar cavities, pulmonary bullae, a large number of inflammatory cell infiltration in the lung tissue, accompanied by severe fibrosis appeared. After YFTBD intervention, the degree of pulmonary fibrosis in mice was significantly improved, inflammatory cell infiltration was reduced, blue collagen deposition in lung interstitial was reduced, pulmonary fibrosis was improved, and lung tissue structure was restored.

The level of lung hydroxyproline is an important index to evaluate the metabolic situation of collagen. Compared with the control group, the level of hydroxyproline in the lung tissue of the model group was significantly increased

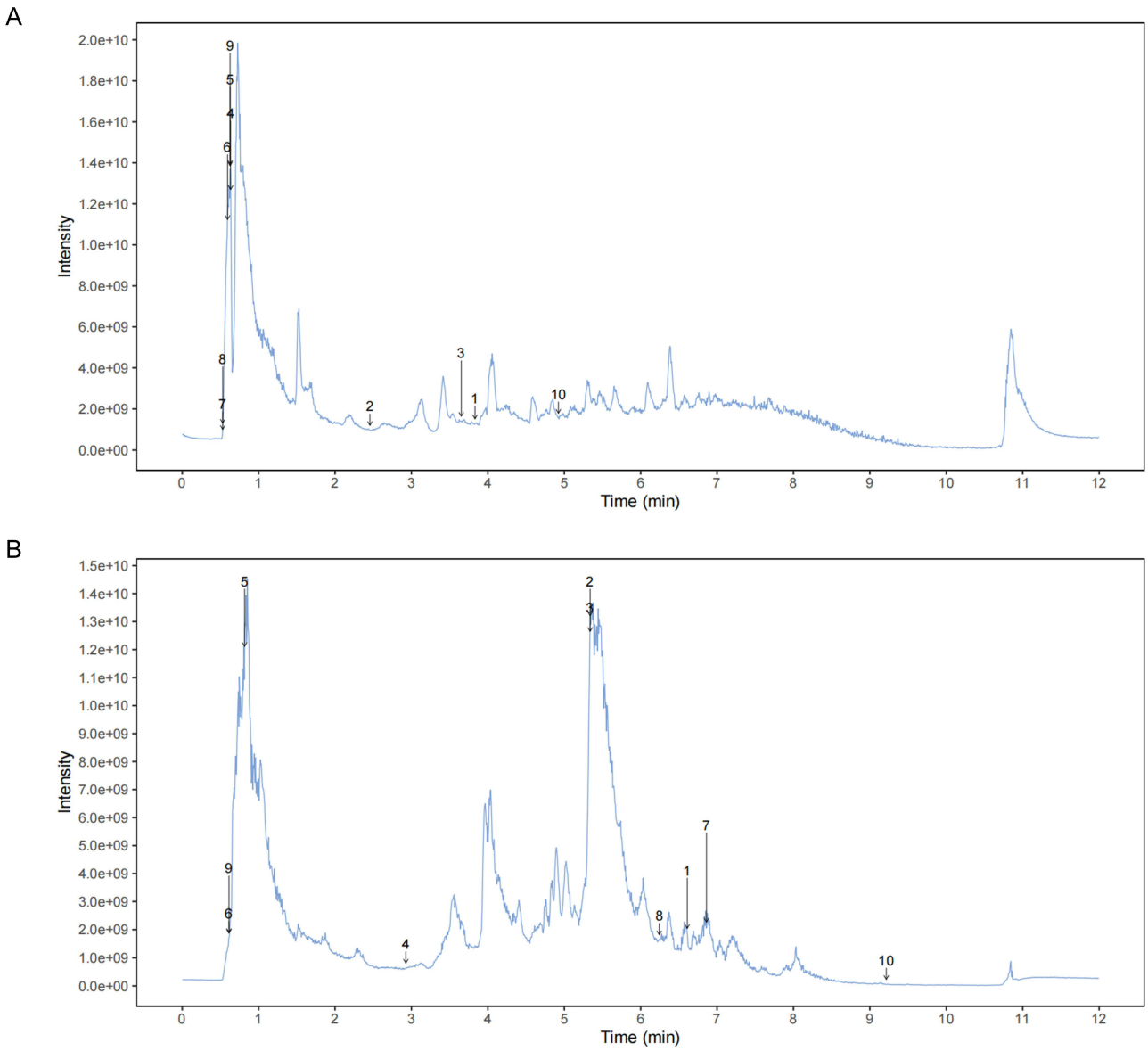

Figure 1 Total ion chromatogram of YFTBD by HPLC-MS. (**A**) Positive ion mode total ion chromatogram. (**B**) Negative ion mode total ion chromatogram.

(Figure 2C, $P < 0.001$). Compared with model group, the level of hydroxyproline in lung tissue of mice in nintedanib group and YFTBD group decreased (Figure 2D, $P < 0.05$).

YFTBD Regulates TGF-β1/Smad Signaling Pathway

α-SMA and TGF-β1 are important factors in pulmonary fibrosis and may be co-involved in its formation. α-SMA is the signature protein of myofibroblasts, and also the basis of myofibroblasts with contractile activity. It is involved in the synthesis of extracellular matrix components such as collagen, and its content can be used as an indirect indicator to determine the degree of pulmonary fibrosis. TGF-β1 activates the TGF-β1/Smad pathway to promote fibrosis. As shown in Figure 3A–F, the results showed that the levels of α-SMA (Figure 3A and B) and TGF-β1 (Figure 3C and D) and in lung tissue of mice induced by bleomycin increased, and YFTBD decreased TGF-β1 (Figure 3C and D) and increase Smad7 (Figure 3E and F) levels. The expression of Smad7 indicates that YFTBD may inhibit the progression of pulmonary fibrosis by regulating TGF-β1/Smad7 signaling pathway.

https://doi.org/10.2147/DDDT.S515368

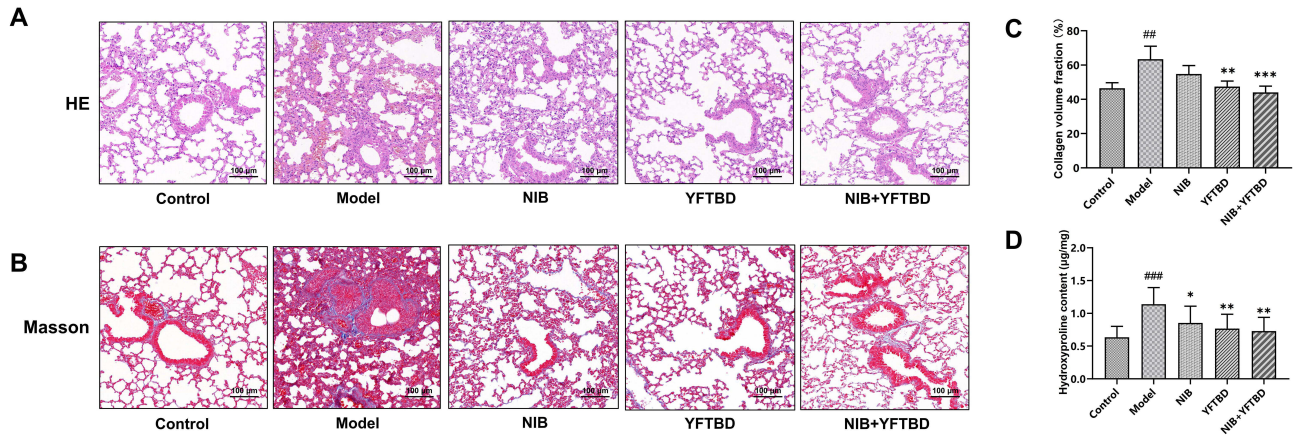

Figure 2 Effects of YFTBD on lung injury and collagen deposition in mice. (**A**) H&E staining of lung tissue. (**B**) Masson staining of lung tissue. (**C**) Collagen volume fraction. n=5. Compared to control, $^{\#\#}P<0.01$. Compared to model, $^{**}P<0.01$, $^{***}P<0.001$. (**D**) Content of hydroxyproline in lung tissue. n=5. Compared to control, $^{\#\#\#\#}P<0.001$. Compared to model, $^{*}P<0.05$, $^{**}P<0.01$.

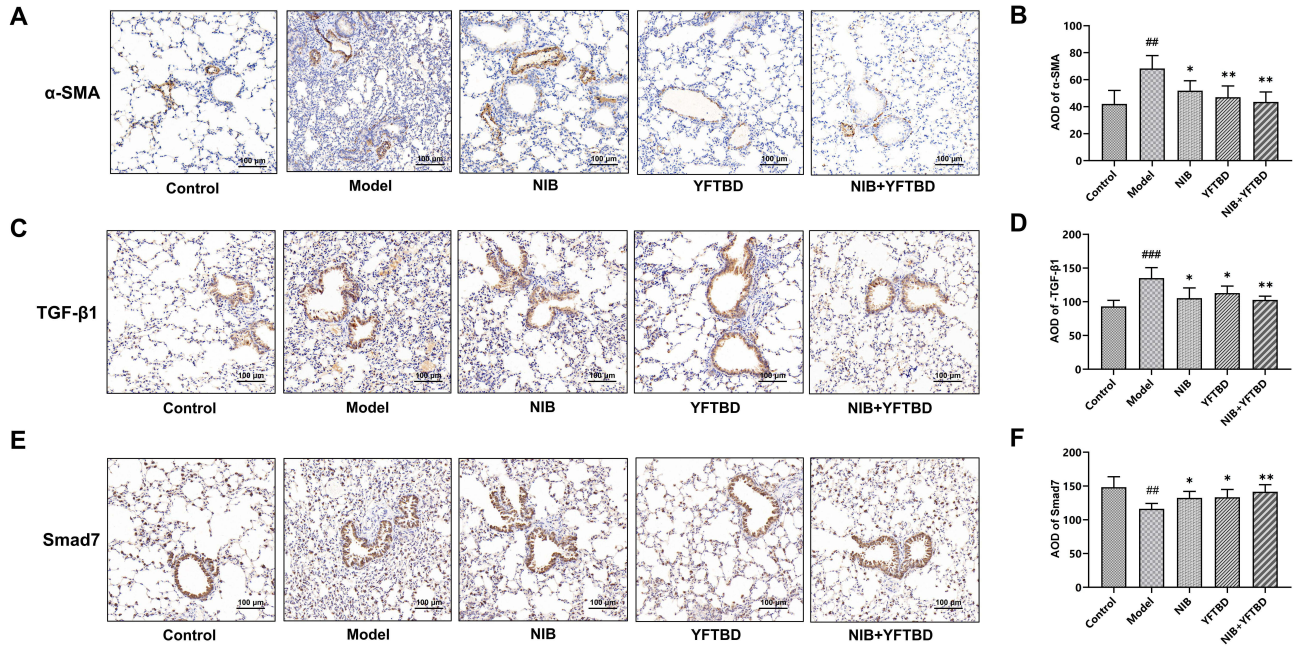

Figure 3 Effects of YFTBD on α-SMA, Smad7, and TGF-β1. (**A**) Immunohistochemistry of α-SMA. (**B**) AOD of α-SMA. n=5. Compared to control, $^{\#\#}P<0.01$. Compared to model, $^{*}P<0.05$, $^{**}P<0.01$. (**C**) Immunohistochemistry of TGF-β1. (**D**) AOD of TGF-β1. n=5. Compared to control, $^{\#\#\#\#}P<0.001$. Compared to model, $^{*}P<0.05$, $^{**}P<0.01$. (**E**) Immunohistochemistry of Smad7. (**F**) AOD of Smad7. n=5. Compared to control, $^{\#\#}P<0.01$. Compared to model, $^{*}P<0.05$, $^{**}P<0.01$.

YFTBD Alleviates Cell Senescence in the Lung Tissue of Mice

A growing number of studies show that the senescence of alveolar epithelial cells promotes the development of pulmonary fibrosis, whereas its inhibition could effectively improve the progression of pulmonary fibrosis.[30–34] It was found that thought upregulating peroxisome proliferator-activated receptor (PPAR)-γ coactivator-1α (PGC-1α) could improve alveolar epithelial cell aging.[35,36] To assess the effect of YFTBD on cell senescence, we measure the levels of senescence markers p21 and p16, and PGC-1α in lung tissues by immunohistochemical staining. The results showed that the expression of p16 (Figure 4A and B) and p21 (Figure 4C and D) and proteins related to cellular senescence in lung tissue of mice in the model group increased. After YFTBD intervention, the cellular senescence in lung tissue of mice was improved, and the expression of p21 and p16 senescence-related proteins was significantly down-regulated. Meanwhile, the expression of PGC-1α (Figure 4E and F) was inhibited in the bleomycin treatment group, and

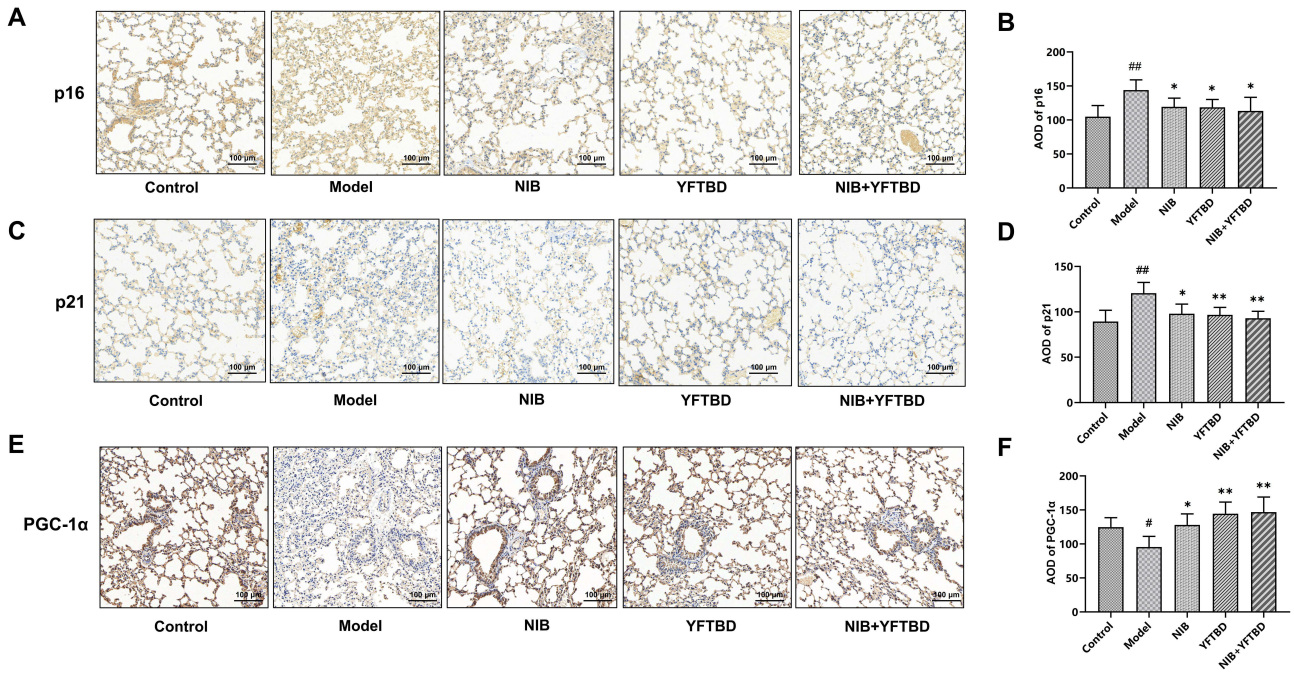

Figure 4 Effects of YFTBD on cell senescence in the lung tissue of mice. (**A**) Immunohistochemistry of p16. (**B**) AOD of p16. n=5. Compared to control, $^{\#\#}P<0.01$. Compared to model, $^{*}P<0.05$. (**C**) Immunohistochemistry of p21. (**D**) AOD of p21. n=5. Compared to control, $^{\#\#}P<0.01$. Compared to model, $^{*}P<0.05$, $^{**}P<0.01$. (**E**) Immunohistochemistry of PGC-1α. (**F**) AOD of PGC-1α. n=5. Compared to control, $^{\#}P<0.05$. Compared to model, $^{*}P<0.05$, $^{**}P<0.01$.

YFTBD could significantly improve its expression and reduce the effect of bleomycin. These results suggest that YFTBD may inhibit cell senescence by regulating p21 signaling pathway, thus delaying the progression of pulmonary fibrosis.

YFTBD Reduces Inflammatory Factor Levels in the Serum of Mice

To reveal the effect of YFTBD on the inflammation in mice, serum IL-1β, IL-6, and TNF-α levels of mice in each group were detected by ELISA. The results showed that compared with the model group, the serum contents of IL-1β (Figure 5A), IL-6 (Figure 5B), and TNF-α (Figure 5C) in the YFTBD and NIB+YFTBD groups were significantly decreased. It is suggested that nintedanib and YFTBD may reduce the inflammatory response induced by bleomycin in mice.

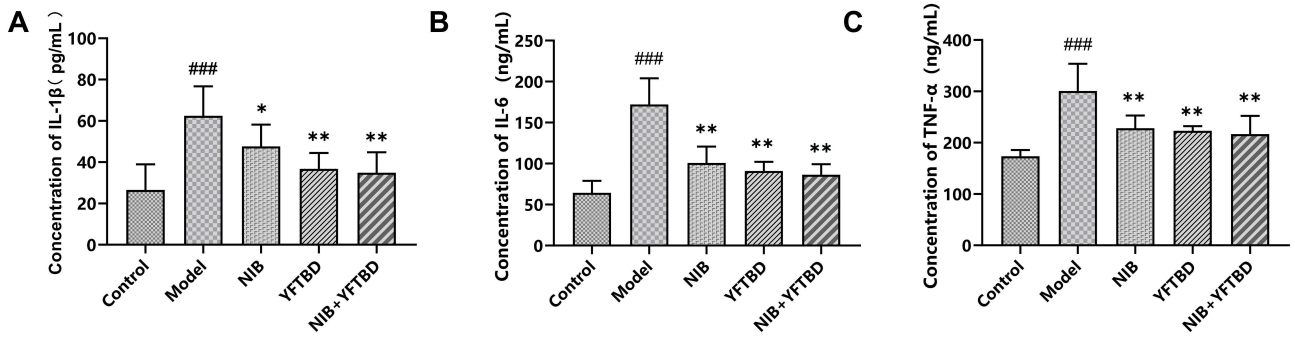

Figure 5 Effects of YFTBD on inflammatory factor levels in the serum of mice. (**A**) Concentration of IL-1β. n=8. Compared to control, $^{\#\#\#}P<0.001$. Compared to model, $^{*}P<0.05$, $^{**}P<0.01$. (**B**) Concentration of IL-6. n=8. Compared to control, $^{\#\#\#}P<0.001$. Compared to model, $^{**}P<0.01$. (**C**) Concentration of TNF-α. n=8. Compared to control, $^{\#\#\#}P<0.001$. Compared to model, $^{**}P<0.01$.

https://doi.org/10.2147/DDDT.S515368

YFTBD Regulates the Gut Microbiota of Mice

One day before the mice were euthanized, feces from each group were collected for 16S rRNA high-throughput sequencing, sequenced based on Illumina Nova sequencing platform, PCR-free library was constructed, and then double-terminal sequencing was performed. The sequences were grouped into Operational Taxonomic Units (OTUs) with 97% agreement, and a total of 36567 OTUs were obtained. The results are shown in Figure 6A, which shows that the gut microbiota of mice in each group has different degrees of difference. YFTBD can increase the OTUs number of gut microbiota in mice. As shown in Figure 6B and C, the α-diversity analysis showed that YFTBD can improve the reduction of gut microbiota diversity induced by bleomycin, particularly at the Chao1 index ($P < 0.001$). It plays an obvious role in increasing the richness of species community. Moreover, as shown in Figure 6D and E, β-diversity analysis showed that YFTBD could improve bleomycin-induced changes in gut microbiota of mice.

From the perspective of microbial species composition richness, as shown in Figure 7A, the phylum level mainly includes 8 dominant genera: *Firmicutes, Bacteroidetes, Proteobacteria, Verrucomicrobiota, Actinobacteria, Epsilonbacteraeota,*

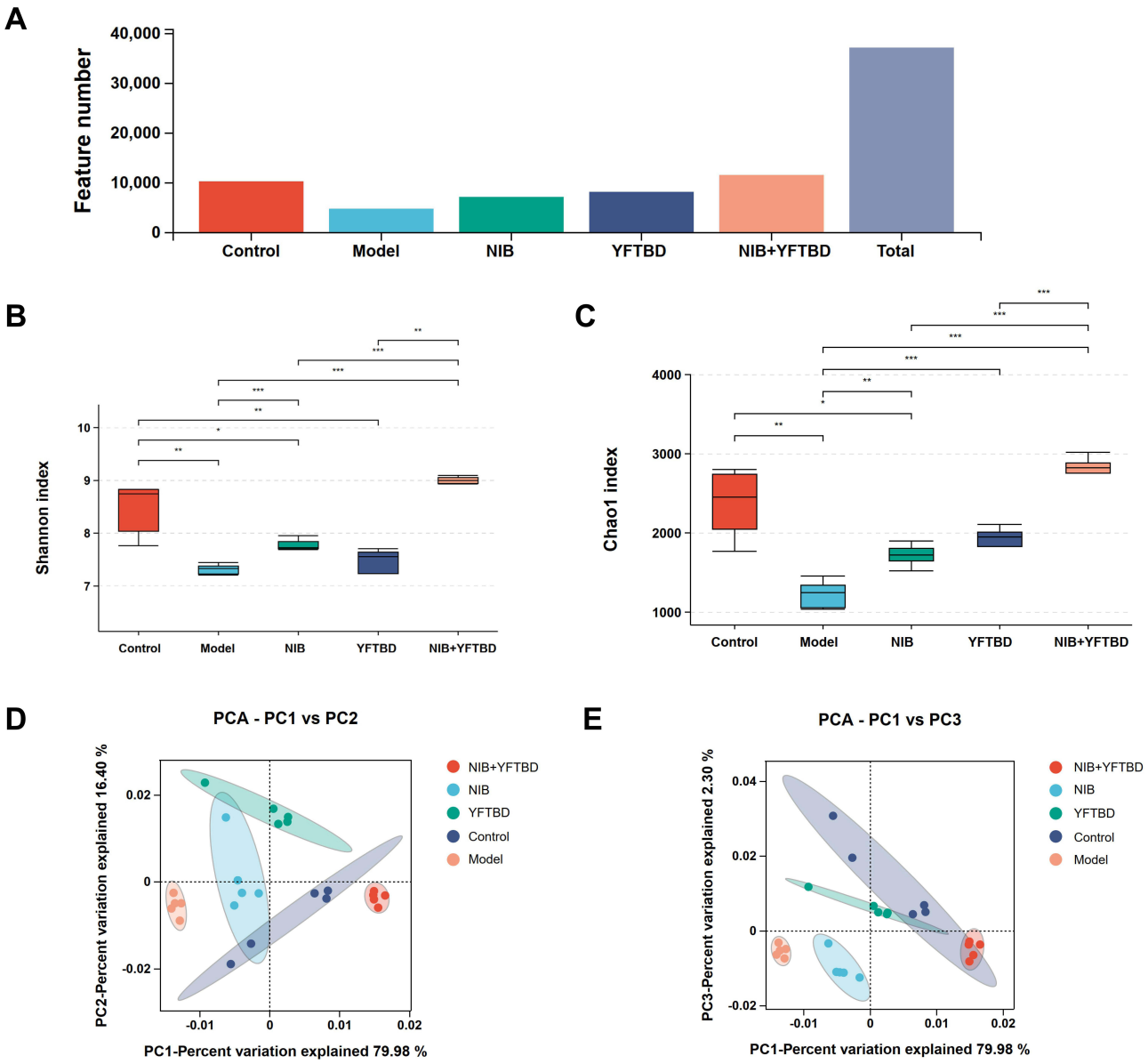

Figure 6 Effects of YFTBD on diversity of gut microbiota in mice. (**A**) OUTs. (**B**) Shannon index. n=5. **P*<0.05, ***P*<0.01, ****P*<0.001. (**C**) Chao1 index. n=5. **P*<0.05, ***P*<0.01, ****P*<0.001. (**D**) Principal component analysis (PC1 vs PC2). (**E**) Principal component analysis (PC1 vs PC3).

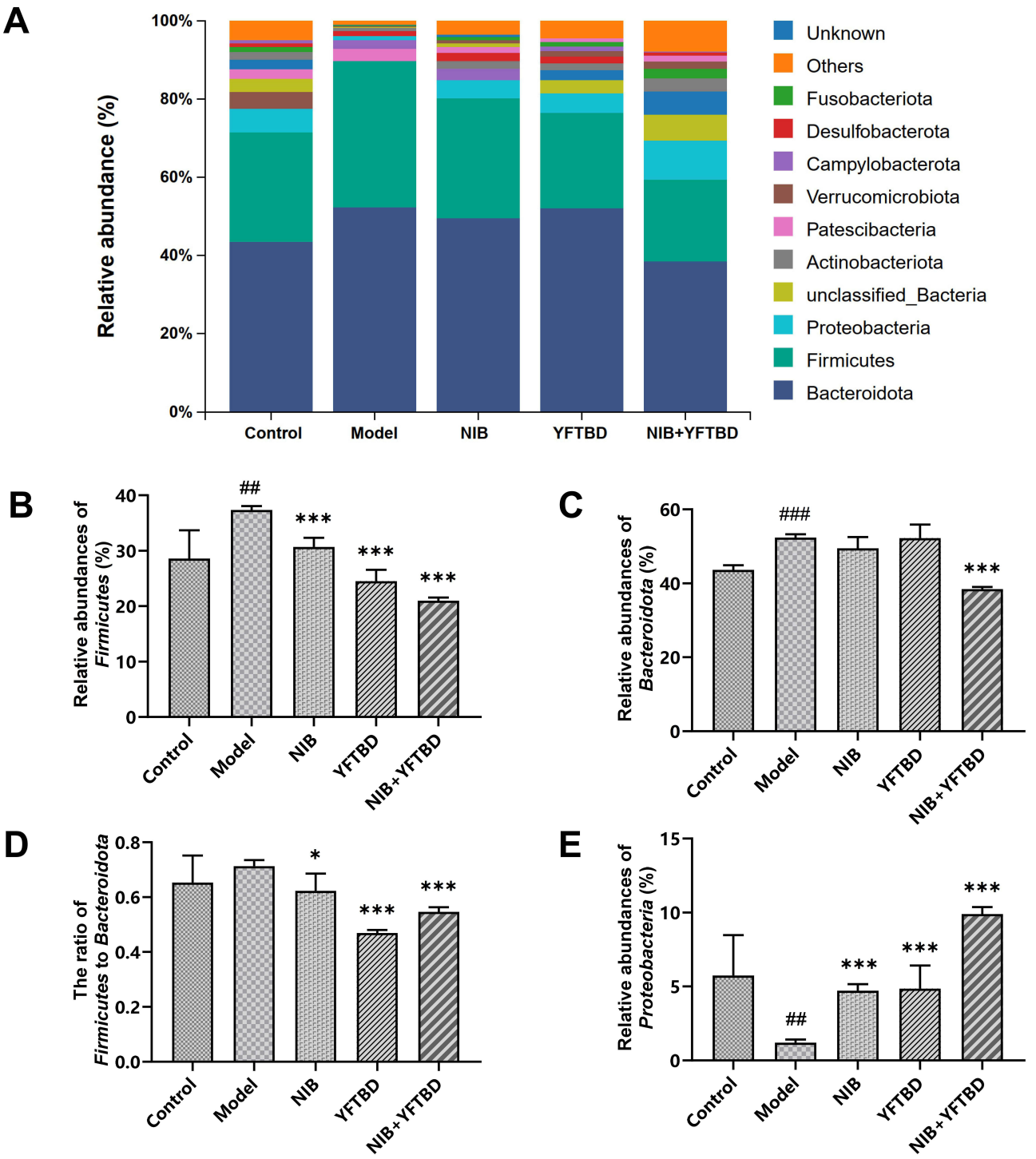

Figure 7 The relative abundance of gut microbiota at the phylum level. (**A**) The histogram of species distribution at the phylum level (n=5). (**B**) Relative abundances of *Firmicutes* (%). n=5. Compared to control, $^{\#\#}P<0.01$. Compared to model, $^{***}P<0.001$. (**C**) Relative abundances of *Bacteroidota* (%). n=5. Compared to control, $^{\#\#\#}P<0.001$. Compared to model, $^{***}P<0.001$. (**D**) The ratio of *Firmicutes* to *Bacteroidota*. n=5. Compared to model, $^{*}P<0.05$, $^{***}P<0.001$. (**E**) Relative abundances of *Proteobacteria* (%). n=5. Compared to control, $^{\#\#}P<0.01$. Compared to model, $^{***}P<0.001$.

Deferribacteres and *Tenericutes*. Among them, *Firmicutes* and *Bacteroidetes* are the two bacterias with the highest relative abundance. Compared with the normal control group, the relative abundance of *Firmicutes* in the model group increases significantly (Figure 7B, $P < 0.001$). Compared with the model group, the relative abundance of *Firmicutes* in YFTBD treated mice decreased significantly ($P < 0.05$). Compared with the model group, there was no significant difference in the relative

https://doi.org/10.2147/DDDT.S515368

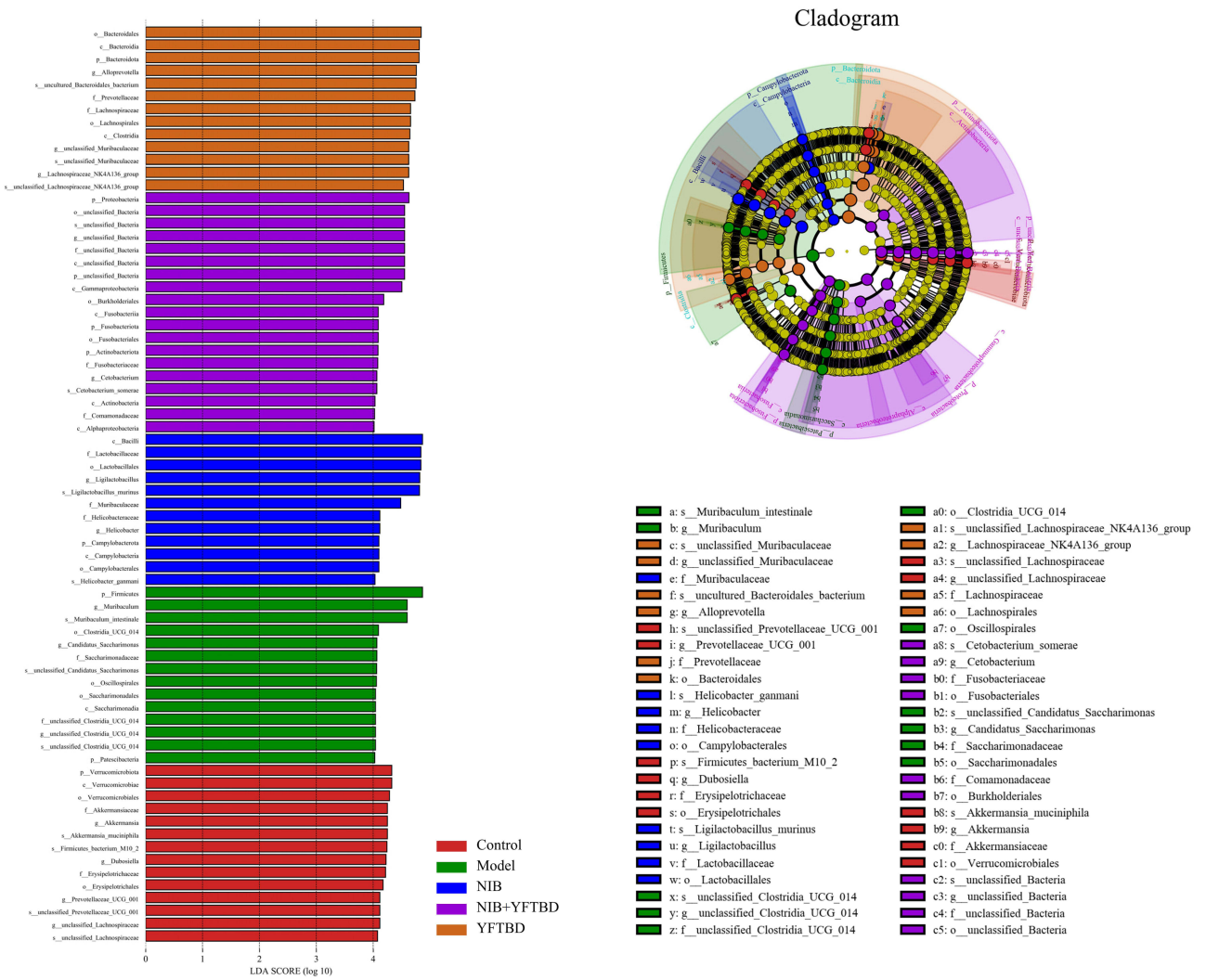

Figure 8 Lefse biomarkers cladogram less strict of the gut microbiota (LDA > 4).

abundance of Firmicutes in mice treated with nintedanib. Moreover, compared with the model group, the relative abundance of *Bacteroidetes* in the YFTBD-treated mice was significantly increased (Figure 7C and 7D, $P < 0.001$). The above results indicate that YFTBD can change the relative abundance of gut microbiota in mice, which may be mainly through changing the ratio of *Firmicutes* and *Bacteroidetes* in mice (Figure 7D), thereby changing the metabolism of intestinal short-chain fat in mice. Particularly, based on the analysis of microflora differences among different groups of samples at the genus level, it was discovered that YFTBD could raise the proportion of bacteria that produced short-chain fatty acid unclassified_*Muribaculaceae* (Figure 7E). Meanwhile, LEfSe, which compares differences between or within groups was conducted to identify significant biomarkers. As shown in Figure 8, it suggests that nintedanib and YFTBD could regulates the phylum, class and order levels of *Bacteroidetes*. However, the role of its active components of YFTBD on regulating gut-lung crosstalk remains unclear, which will be the focus of our future studies.

Discussion

Pulmonary fibrosis leads to respiratory failure, resulting in a high disability rate and mortality of patients.[37,38] YFTBD is the commonly used empirical prescription in the treatment of interstitial pulmonary disease, which can significantly improve the respiratory symptoms of patients with idiopathic pulmonary fibrosis such as cough and shortness of breath. At present, the main first-line drugs for pulmonary fibrosis are pirfenidone and nintedanib, but there are adverse reactions

such as nausea, vomiting and photoallergy, which seriously affect the quality of life of patients. So further explore YFTBD on the pharmacological mechanism of pulmonary fibrosis has very important significance.

Recent studies have shown that gut microbiota are closely related to and interact with the pathological changes of the respiratory tract, which is involved in the occurrence and development of a variety of lung diseases, including asthma, lung cancer, chronic obstructive pulmonary disease, acute lung injury and pulmonary fibrosis.[23] The diversity of gut microbiota is the basis for promoting the absorption of nutrients and maintaining the body's immunity and metabolism. The changes in the structure, species, function of gut microbiota and the metabolites produced by gut microbiota play an important role in the improvement of pulmonary fibrosis.[39] The results of this study showed that compared with the control group, the α diversity and β diversity of gut microbiota in the model group were different to some extent, and Firmicutes/Bacteroides were increased, indicating that the gut microbiota structure and flora species of mice with pulmonary fibrosis were changed. The diversity of gut microbiota in YFTBD group and NIB+YFTBD group was close to that in the control group, suggesting that YFTBD could alleviate the gut microbiota disturbance caused by bleomycin, and Firmicutes/Bacteroidetes were lower than those in the model group. This indicates that YFTBD can improve Firmicutes/Bacteroidetes imbalance, and can regulate pulmonary inflammatory and immune responses through the lung-intestinal axis, affecting the progression of pulmonary fibrosis.

Nintedanib is an intracellular inhibitor that targets multiple tyrosine kinases,[40] which can reduce bleomycin-induced inflammation by downregulating PI3K/Akt/mTOR pathway, pulmonary fibrosis, and oxidative stress.[41] However, clinical studies have shown that diarrhea is the most common adverse event during.[8,42] Study have shown that the nintedanib improved the composition of the gut microbiota in mice with DSS-induced experimental colitis.[43] In this study, our results also showed that nintedanib could improve bleomycin-induced pulmonary fibrosis in mice and had the effect of regulating gut microbiota. Especially, our results suggest that the combination of nintedanib and YFTBD might provide additive effects on bleomycin-induced pulmonary fibrosis in mice compared with either monotherapy.

Conclusion

In conclusion, YFTBD alleviate the bleomycin-induced pulmonary fibrosis in mice. The therapeutic mechanism of YFTBD is related to regulating TGF-β1/Smad signaling pathway, inflammation and gut microbiota, and it needs further study.

Abbreviations

AOD, average optical density; DSS, dextran sulfate sodium; ELISA, Enzyme-Linked Immunosorbent Assay; HPLC, high performance liquid chromatography; LDA, Linear discriminant analysis; LEfSe, Linear discriminant analysis effect size; MS, mass spectrometry; NIB, nintedanib; PPAR, peroxisome proliferator-activated receptor; PGC-1α, Peroxisome proliferator-activated receptor γ coactivator 1-α; TCM, traditional Chinese medicine; TIC, total ion chromatogram; YFTBD, Yi-Fei-Tong-Bi decoction.

Data Sharing Statement

The data will be made available upon request from the corresponding author.

Ethics Approval

The research was conducted in accordance with the internationally accepted principles for laboratory animal use and care as found in for example the European Community guidelines (EEC Directive of 1986; 86/609/EEC) or the US guidelines (NIH publication no. 85-23, revised in 1985). The animal experiments were reviewed and approved by the Ethics Committee of the Chongqing Academy of Chinese Materia Medica.

Author Contributions

All authors made a significant contribution to the work reported, whether that is in the conception, study design, execution, acquisition of data, analysis and interpretation, or in all these areas; took part in drafting, revising or critically

reviewing the article; gave final approval of the version to be published; have agreed on the journal to which the article has been submitted; and agree to be accountable for all aspects of the work.

Funding

This research was supported by Science and Technology Innovation Key R&D Program of Chongqing (CSTB2024TIAD-STX0041), grants from the Program for the key projects of the Chongqing Science and Health Joint Traditional Chinese Medicine Research Project (2024ZYZD007), and funds from the Chongqing Science and Technology Commission (cstc2023jxjl-jbky130009), Chongqing Municipal Health Commission, grant number [2021] 16; Chongqing Agriculture Commission, grant number 2022 [10]; Chongqing Supervision Bureau, grant number CQBD 2021-0079.

Disclosure

The authors report no conflicts of interest in this work.

References

1. Koudstaal T, Funke-Chambour M, Kreuter M, Molyneaux PL, Wijsenbeek MS. Pulmonary fibrosis: from pathogenesis to clinical decision-making. *Trends Mol Med*. 2023;29(12):1076–1087. doi:10.1016/j.molmed.2023.08.010
2. Richeldi L, Collard HR, Jones MG. Idiopathic pulmonary fibrosis. *Lancet*. 2017;389(10082):1941–1952. doi:10.1016/S0140-6736(17)30866-8
3. Maher TM. Interstitial Lung Disease: a Review. *JAMA*. 2024;331(19):1655–1665. doi:10.1001/jama.2024.3669
4. Zhao C, Yin Y, Zhu C, et al. Drug therapies for treatment of idiopathic pulmonary fibrosis: a systematic review, Bayesian network meta-analysis, and cost-effectiveness analysis. *EClinicalMedicine*. 2023;61:102071. doi:10.1016/j.eclinm.2023.102071
5. Flaherty KR, Wells AU, Cottin V, et al. Nintedanib in progressive fibrosing interstitial lung diseases. *N Engl J Med*. 2019;381(18):1718–1727. doi:10.1056/NEJMoa1908681
6. Kim JS, Murray S, Yow E, et al. Comparison of Pirfenidone and Nintedanib: post Hoc Analysis of the CleanUP-IPF Study. *Chest*. 2024;165(5):1163–1173. doi:10.1016/j.chest.2023.11.035
7. Solomon JJ, Danoff SK, Woodhead FA, et al. Safety, tolerability, and efficacy of pirfenidone in patients with rheumatoid arthritis-associated interstitial lung disease: a randomised, double-blind, placebo-controlled, Phase 2 study. *Lancet Respir Med*. 2023;11(1):87–96. doi:10.1016/S2213-2600(22)00260-0
8. Richeldi L, Du Bois RM, Raghu G, et al. Efficacy and safety of nintedanib in idiopathic pulmonary fibrosis. *N Engl J Med*. 2014;370(22):2071–2082. doi:10.1056/NEJMoa1402584
9. Bai Y, Li J, Zhao P, et al. A Chinese Herbal Formula Ameliorates Pulmonary Fibrosis by Inhibiting Oxidative Stress via Upregulating Nrf2. *Front Pharmacol*. 2018;9:628. doi:10.3389/fphar.2018.00628
10. Chu H, Shi Y, Jiang S, et al. Treatment effects of the traditional Chinese medicine Shenks in bleomycin-induced lung fibrosis through regulation of TGF-beta/Smad3 signaling and oxidative stress. *Sci Rep*. 2017;7(1):2252. doi:10.1038/s41598-017-02293-z
11. Hao Y, Li J, Dan L, et al. Chinese medicine as a therapeutic option for pulmonary fibrosis: clinical efficacies and underlying mechanisms. *J Ethnopharmacol*. 2024;318(Pt A):116836. doi:10.1016/j.jep.2023.116836
12. Khazri O, Mezni A, Limam F, Ezzeddine A. Bleomycin-Induced Damage in Rat Lung: protective Effect of Grape Seed and Skin Extract. *Dose Response*. 2022;20(4):15593258221131648. doi:10.1177/15593258221131648
13. Qin S, Tan P, Xie J, Zhou Y, Zhao J. A systematic review of the research progress of traditional Chinese medicine against pulmonary fibrosis: from a pharmacological perspective. *Chin Med*. 2023;18(1):96. doi:10.1186/s13020-023-00797-7
14. Shi W, Feng B, Xu S, Shen X, Zhang T. Inhibitory effect of compound Chuanxiong Kangxian granules on bleomycin-induced pulmonary fibrosis in rats. *Biomed Pharmacother*. 2017;96:1179–1185. doi:10.1016/j.biopha.2017.11.104
15. Wang L, Li S, Yao Y, Yin W, Ye T. The role of natural products in the prevention and treatment of pulmonary fibrosis: a review. *Food Funct*. 2021;12(3):990–1007. doi:10.1039/D0FO03001E
16. Zhao F, Shi D, Li T, Li L, Zhao M. Silymarin attenuates paraquat-induced lung injury via Nrf2-mediated pathway in vivo and in vitro. *Clin Exp Pharmacol Physiol*. 2015;42(9):988–998. doi:10.1111/1440-1681.12448
17. Shao R, Wang FJ, Lyu M, Yang J, Zhang P, Zhu Y. Ability to Suppress TGF-β-Activated Myofibroblast Differentiation Distinguishes the Anti-pulmonary Fibrosis Efficacy of Two Danshen-Containing Chinese Herbal Medicine Prescriptions. *Front Pharmacol*. 2019;10:412. doi:10.3389/fphar.2019.00412
18. Liu B, Lü W, Ge H, Tang H, Li R, Zhang C. Protective Effect of the Traditional Chinese Patent Medicine Qing-Xuan Granule against Bleomycin-Induced Pulmonary Fibrosis in Mice. *Chem Biodivers*. 2019;16(12):e1900467. doi:10.1002/cbdv.201900467
19. Yang JY, Tao LJ, Liu B, et al. Wedelolactone Attenuates Pulmonary Fibrosis Partly Through Activating AMPK and Regulating Raf-MAPKs Signaling Pathway. *Front Pharmacol*. 2019;10:151. doi:10.3389/fphar.2019.00151
20. Yin ZF, Wei YL, Wang X, Wang LN, Li X. Buyang Huanwu Tang inhibits cellular epithelial-to-mesenchymal transition by inhibiting TGF-β1 activation of PI3K/Akt signaling pathway in pulmonary fibrosis model in vitro. *BMC Complement Med Ther*. 2020;20(1):13. doi:10.1186/s12906-019-2807-y
21. Shuangshuang H, Mengmeng S, Lan Z, Fang Z, Yu L. Maimendong decoction regulates M2 macrophage polarization to suppress pulmonary fibrosis via PI3K/Akt/FOXO3a signalling pathway-mediated fibroblast activation. *J Ethnopharmacol*. 2024;319(Pt 3):117308. doi:10.1016/j.jep.2023.117308
22. Qin H, Wen HT, Gu KJ, et al. Total extract of Xin Jia Xuan Bai Cheng Qi decoction inhibits pulmonary fibrosis via the TGF-β/Smad signaling pathways in vivo and in vitro. *Drug Des Devel Ther*. 2019;13:2873–2886. doi:10.2147/DDDT.S185418

23. Sun M, Lu F, Yu D, Wang Y, Chen P, Liu S. Respiratory diseases and gut microbiota: relevance, pathogenesis, and treatment. *Front Microbiol*. 2024;15:1358597. doi:10.3389/fmicb.2024.1358597
24. Dong Y, He L, Zhu Z, et al. The mechanism of gut-lung axis in pulmonary fibrosis. *Front Cell Infect Microbiol*. 2024;14:1258246. doi:10.3389/fcimb.2024.1258246
25. Luo T, Che Q, Guo Z, Song T, Zhao J, Xu D. Modulatory effects of traditional Chinese medicines on gut microbiota and the microbiota-gut-x axis. *Front Pharmacol*. 2024;15:1442854. doi:10.3389/fphar.2024.1442854
26. Gu X, Wei W, Liu Z, et al. Assessment of traditional Chinese medicine pattern in a bleomycin-induced pulmonary fibrosis mouse model: a pilot study. *J Tradit Chin Med Sci*. 2022;9(4):400–408. doi:10.1016/j.jtcms.2022.09.005
27. Xu Y, Peng W, Han D, et al. Maiwei Yangfei decoction prevents bleomycin-induced pulmonary fibrosis in mice. *Exp Ther Med*. 2021;22(5):1306. doi:10.3892/etm.2021.10741
28. Shin H, Park S, Hong J, et al. Overexpression of fatty acid synthase attenuates bleomycin induced lung fibrosis by restoring mitochondrial dysfunction in mice. *Sci Rep*. 2023;13(1):9044. doi:10.1038/s41598-023-36009-3
29. Li N, Wang D, Wen X, et al. Effects of polysaccharides from *Gastrodia elata* on the immunomodulatory activity and gut microbiota regulation in cyclophosphamide-treated mice. *J Sci Food Agric*. 2023;103(7):3390–3401. doi:10.1002/jsfa.12491
30. Xie W, Deng L, Zhang X, et al. Myricetin Alleviates Silica-Mediated Lung Fibrosis via PPARγ-PGC-1α Loop and Suppressing Mitochondrial Senescence in Epithelial Cells. *J Agric Food Chem*. 2024;72(50):27737–27749. doi:10.1021/acs.jafc.4c04887
31. Summer R, Shaghaghi H, Schriner D, et al. Activation of the mTORC1/PGC-1 axis promotes mitochondrial biogenesis and induces cellular senescence in the lung epithelium. *Am J Physiol Lung Cell mol Physiol*. 2019;316(6):L1049–L1060. doi:10.1152/ajplung.00244.2018
32. Zhuo J, Chu L, Liu D, et al. Tetrandrine Alleviates Pulmonary Fibrosis by Modulating Lung Microbiota-Derived Metabolism and Ameliorating Alveolar Epithelial Cell Senescence. *Phytother Res*. 2025;39(1):298–314. doi:10.1002/ptr.8374
33. Hernandez-Gonzalez F, Pietrocola F, Cameli P, et al. Exploring the Interplay between Cellular Senescence, Immunity, and Fibrosing Interstitial Lung Diseases: challenges and Opportunities. *Int J mol Sci*. 2024;25(14):7554. doi:10.3390/ijms25147554
34. Qi Z, Yang W, Xue B, et al. ROS-mediated lysosomal membrane permeabilization and autophagy inhibition regulate bleomycin-induced cellular senescence. *Autophagy*. 2024;20(9):2000–2016. doi:10.1080/15548627.2024.2353548
35. Zeng Q, Luo Y, Sang X, et al. Senegenin Attenuates Pulmonary Fibrosis by Inhibiting Oxidative-Stress-Induced Epithelial Cell Senescence through Activation of the Sirt1/Pgc-1α Signaling Pathway. *Antioxidants*. 2024;13(6):1.
36. Ma M, Gao Y, Qiu X, et al. ZLN005 improves the protective effect of mitochondrial function on alveolar epithelial cell aging by upregulating PGC-1α. *J Thorac Dis*. 2023;15(11):6160–6177. doi:10.21037/jtd-23-815
37. Mena-Vázquez N, Redondo-Rodriguez R, Rojas-Gimenez M, et al. Rate of severe and fatal infections in a cohort of patients with interstitial lung disease associated with rheumatoid arthritis: a multicenter prospective study. *Front Immunol*. 2024;15:1341321. doi:10.3389/fimmu.2024.1341321
38. Fidler L, Widdifield J, Fisher J, Shapera S, Gershon AS. Early versus late onset interstitial lung disease in rheumatoid arthritis: an observational study of risk factors and mortality in Ontario, Canada. *Respirology*. 2024;29(3):243–251. doi:10.1111/resp.14645
39. Hou S, Wang X, Guo J, et al. Triangle correlations of lung microbiome, host physiology and gut microbiome in a rat model of idiopathic pulmonary fibrosis. *Sci Rep*. 2024;14(1):28743. doi:10.1038/s41598-024-80023-y
40. Lamb YN. Nintedanib: a Review in Fibrotic Interstitial Lung Diseases. *Drugs*. 2021;81(5):575–586. doi:10.1007/s40265-021-01487-0
41. Pan L, Cheng Y, Yang W, et al. Nintedanib Ameliorates Bleomycin-Induced Pulmonary Fibrosis, Inflammation, Apoptosis, and Oxidative Stress by Modulating PI3K/Akt/mTOR Pathway in Mice. *Inflammation*. 2023;46(4):1531–1542. doi:10.1007/s10753-023-01825-2
42. Distler O, Highland KB, Gahlemann M, et al. Nintedanib for Systemic Sclerosis-Associated Interstitial Lung Disease. *N Engl J Med*. 2019;380(26):2518–2528. doi:10.1056/NEJMoa1903076
43. Li H, Li J, Xiao T, et al. Nintedanib Alleviates Experimental Colitis by Inhibiting CEBPB/PCK1 and CEBPB/EFNA1 Pathways. *Front Pharmacol*. 2022;13:904420. doi:10.3389/fphar.2022.904420